Aalborg Universitet

AALBORG UNIVERSITY

Computational fluid dynamics predictions of non-isothermal ventilation flow—How can the user factor be minimized?

van Hooff, Twan; Nielsen, Peter V.; Li, Yuguo

ORIGINAL ARTICLE

WILEY

Computational fluid dynamics predictions of non-isothermal ventilation flow—How can the user factor be minimized?

Twan van Hooff[1,2] 🆔 | Peter V. Nielsen[3] | Yuguo Li[4] 🆔

[1]Department of Civil Engineering, KU Leuven, Leuven, Belgium

[2]Department of the Built Environment, Eindhoven University of Technology, Eindhoven, The Netherlands

[3]Department of Civil Engineering, Aalborg University, Aalborg, Denmark

[4]Department of Mechanical Engineering, The University of Hong Kong, Pokfulam, Hong Kong Special Administrative Region, China

Correspondence: Twan van Hooff, Building Physics Section, Department of Civil Engineering, KU Leuven, Kasteelpark Arenberg 40—box 2447, 3001 Leuven, Belgium (twan.vanhooff@kuleuven.be).

Abstract

The use of computational fluid dynamics (CFD) to solve indoor airflow problems has increased tremendously in the last decades. However, the accuracy of CFD simulations depends greatly on user experience, the available validation data, and the effort made to verify solutions. This study presents the results of a conference workshop, which assessed user influence on the CFD results obtained for a generic non-isothermal flow problem; ie, a backward-facing step flow problem with a heated wall below the supply. Fifty-five simulation sets were submitted by 32 teams. The results showed a very large spread in predicted penetration length ($x_{re}/(H - h)$), location of maximum velocity in the lower part of the recirculation cell ($x_{rm}/(H - h)$), and maximum velocity at this location (u_{rm}/u_0). The turbulence model seemed to very strongly influence the results, with a statistically significant difference in the predictions yielded by the k-ε and k-ω models. The results obtained using a single turbulence model generally also showed a spread in results; the level of spread depended on factors such as grid size and near-wall treatment. The statistical data strongly indicate the need for validation studies using experimental data (benchmarks) to ensure the accuracy, reliability, and trustworthiness of CFD simulations for indoor airflow problems.

KEYWORDS
computational fluid dynamics, guidelines, non-isothermal indoor airflow, statistical analysis, user influence, validation and verification

1 | INTRODUCTION

Since the introduction of computational fluid dynamics (CFD) in the 1970s, the use of this tool both in general and for indoor airflow studies in particular has massively increased.[1-8] CFD is a very powerful tool that enables very detailed predictions of airflow and heat and mass transfer in the built environment. Numerous developments have been made in the last few decades. Various turbulence models were introduced in the 1990s, such as advanced versions of the standard k-ε model (eg, RNG,[9] the realizable k-ε model,[10] and low Reynolds number versions). Furthermore, the k-ω model has been

refined and adjusted,[11,12] and higher-order discretization schemes have been developed. Ever-increasing computer power is also important, allowing for higher grid resolutions and the use of low Reynolds number modeling (LRNM) instead of wall functions in the near-wall region, even for more complex geometries. Despite these developments, however, the quality of CFD simulations is still heavily dependent on the user, who has to make numerous decisions on the input to the CFD model. The user must choose between numerous turbulence models, each with its own advantages and disadvantages, different ways of accounting for near-wall flow and different discretization schemes. Convergence has to be judged, and the grid

resolution has to be determined based on not only accuracy but also computational demand. All of these choices can and do affect the outcome of the simulations and thus the quality and reliability of the results. Therefore, procedures for verifying and validating CFD simulations are of the utmost importance. Proper verification and validation should ensure that the equations have been solved correctly (verification) and that the right equations have been solved (validation).[13]

Issues relating to the uncertainty of CFD predictions have been discussed frequently since the early 1990s by researchers such as Roache,[13,14] Stern et al,[15] Oberkampf et al,[16] and Celik et al.[17] Several sets of guidelines have been published to help reduce uncertainty by providing examples and background information on turbulence models, discretization schemes, etc. For example, the Special Interest Group on Quality and Trust in Industrial CFD of the European Research Community on Flow, Turbulence and Combustion (ERCOFTAC) published general guidelines on the use of CFD in industrial contexts.[18] Several similar sets of guidelines on the modeling of indoor airflow have been published in the last 25 years.[4,19–22] The Federation of European Heating, Ventilation and Air Conditioning Associations (REHVA) Guide Book 10 by Nielsen et al[22] provides a comprehensive overview of CFD theory and guidelines for the use of CFD for ventilation design. However, both the extent to which such guidelines are used by the CFD community and their power to limit users' influence on CFD results remain unclear; even more importantly, how significant is the influence of the user on CFD results?

In a review of 30 years of CFD development and application at Boeing, Johnson et al[23] stated that CFD codes "must be very user oriented" and allow "the expert user" to rapidly obtain "results with reduced variation." This emphasis on reducing variation in results is intriguing. To assess the variation in their CFD results, participants in several workshops were asked to perform CFD simulations for given flow problems. Experimental data (benchmark data) on the problems were made available before or after the workshops.[24,25] These comparisons provided valuable information on the sources of errors and uncertainties in CFD simulations of problems relating to combustion,[26] hydrogen energy,[27] and channel flow.[28] Another new method of assessing the errors and uncertainties in the use of CFD, with a focus on the influence of the user, involves providing a flow problem for which no experimental data are available. This new method was first used in a workshop at the International Symposium on Heating, Ventilation and Air Conditioning—Conference on Building Energy and Environment (ISHVAC-COBEE) 2015 in Tianjin, China.[29] Numerous researchers were asked to perform simulations of an isothermal backward-facing step flow for a range of Reynolds numbers (1-10 000), after which the results submitted by the participants were compared. The advantage of the applied methodology (no benchmark data available) is that participants cannot work toward a certain solution. Furthermore, a spread in measurement results may arise, making a fair comparison with the numerical results very difficult and ambiguous. In addition, the participants may be discouraged

Practical Implications

Computational fluid dynamics (CFD) can be a very powerful tool to analyze indoor airflows and heat and mass transfer. The results presented in this study indicate that a very large spread can be present in the results obtained by different researchers for an identical non-isothermal indoor airflow problem. These findings illustrate the need for validation studies using experimental data to ensure the accuracy, reliability, and trustworthiness of CFD for indoor environment studies. If no validation data are available, subconfiguration validation should be performed using experimental data for a similar flow problem.

by deviations between their numerical simulations and the experimental data. The new method enabled the assessment of the spread in the results of CFD simulations of a flow problem that could not be validated due to a lack of experimental data, which is unfortunately often the case in CFD research and practice in the field of indoor airflows and in general. The participants had to rely on their past experience and the literature; however, they could also choose to perform a validation study for a similar flow configuration. Note that although the approach used in such a workshop is useful for assessing the variability of predictions as a result of user influence, it is not recommended for use in other CFD studies, for which solution verification and validation are imperative to demonstrate the accuracy and trustworthiness of the results. Unfortunately, the sample used by Peng et al[29] was too small to cover fully developed turbulent flows; most of the data were on transitional flows.

This study presents the results of a follow-up workshop held at the Indoor Air Conference in 2016 in Ghent, Belgium. As in the workshop run by Peng et al,[29] no benchmark data were available for comparison; however, the prediction of non-isothermal flows was assessed here, by comparing the results submitted by 32 teams. The larger sample used in the workshop reported here also allowed some statistical analysis to be performed, which was not possible for Peng et al.[29] The teams were again free to choose their models, numerical schemes, etc. Please note that the aim was certainly not to assess the errors of the CFD simulations conducted by the participants, which would have been practically impossible due to the lack of experimental data, but to try to find answers to the following questions for a non-isothermal flow problem ($0 < Ar < 8$): (a) What decisions/choices are made by participants when constructing a CFD model? (b) How do these decisions/choices affect the results (eg, what is the influence of turbulence model, near-wall treatment, grid size, what other aspects significantly influence the results? (c) How large is the spread in results due to user-dependent choices? (d) How can we avoid a large spread in the results of CFD simulations for which no
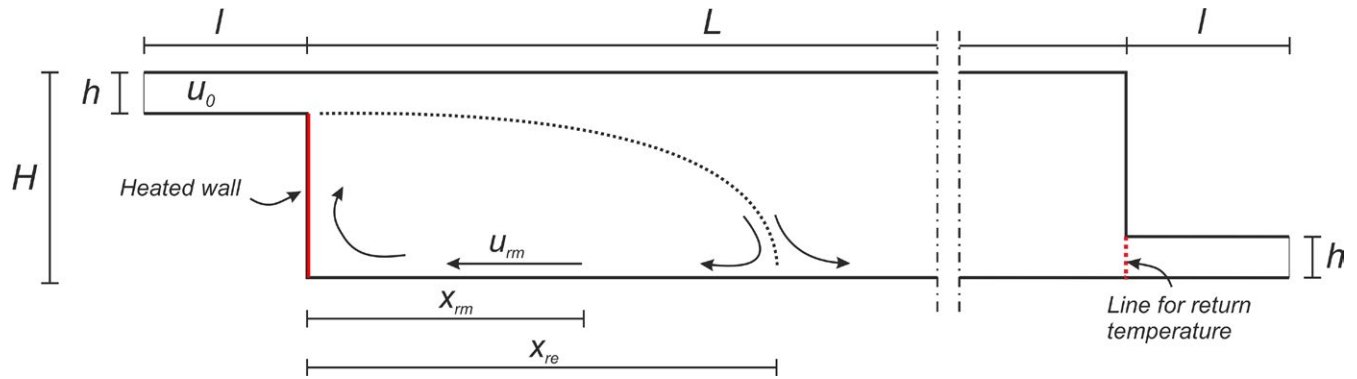
FIGURE 1 Geometry of the test case. The solid red vertical line indicates a heated wall. The dashed red line indicates the location where the return temperature should be taken

experimental data are available? (e) What procedures can reduce the spread in CFD results for indoor airflow problems and thus build confidence in CFD simulations?

Section 2 of this article details the methodology, and the results are presented in Section 3. Section 4, which concludes the article, offers a discussion of the results presented in Section 3. Section 4 is partly based on the discussion during the workshop at the conference in 2016.

2 | METHODOLOGY

2.1 | Flow problem specification

Whereas Peng et al[29] focused on transitional flows, the workshop reported here emphasized non-isothermal turbulent flows in a generic enclosure for a range of Archimedes numbers. The flow was incompressible and two-dimensional (2D) at low Archimedes numbers, but not necessarily across the whole regime. It could be considered a simple building ventilation problem, and its geometry resembled that of the isothermal ISHVAC-COBEE case from 2015;[29] that is, it was a backward-facing step problem. However, thermal effects were included and the length of the enclosure was selected to facilitate the detachment of the wall jet and its reattachment to the bottom surface. The proposed flow problem did not impose an excessively high computational demand due to its assumed two-dimensionality; a personal computer was expected to suffice for the simulations.

2.1.1 | Geometry

Figure 1 shows the geometry of the proposed case. The flow indicated was typical of an isothermal 2D room airflow in a deep room, but non-isothermal effects altered the flow pattern. The parameters H, L, h and l in Figure 1 denote room height, room length, supply slot height, and length of supply opening, respectively, and l and h are the dimensions of the outlet opening as well. The geometry of the case can be described by the following ratios: $h/H = 1/5$, $l/h = 4$ and $L = 10H$. The following combination of the physical dimensions of the problem was suggested to the workshop participants: $H = 5$ m,

$L = 50$ m, $h = 1$ m, $l = 4$ m, $u_0 = 0.16$ m/s, where u_0 is the inlet velocity. As the flow was potentially unsteady and three-dimensional (3D) within a certain range of Archimedes numbers, the 3D geometry was defined by a width (W) of $2H$. In the 3D case, the parameters of interest had to be considered in the vertical median plane, that is, at $y = 0.5W$.

2.1.2 | Boundary conditions

The vertical wall below the supply opening was a heated wall in the non-isothermal predictions (Ar ≠ 0) (see red line in Figure 1). All walls other than the heated wall were adiabatic ($\partial T/\partial n = 0.0$). At low Archimedes numbers, the left side of the model was comparable with the flow problem studied in the ISHVAC-COBEE 2015 workshop,[29] as the room was long (large L). The small return opening ensured that a downstream reverse flow was impossible in the case of large temperature differences.

The inlet flow had a top-hat profile with a constant and uniform velocity u_0. The turbulence variables were specified as 10% turbulent intensity and a viscosity ratio of $\nu_t/\nu = 10$ at the inlet. The Reynolds number was defined as Re $= u_0 h/\nu$, with ν the kinematic viscosity. The value of Re should be 10 000, based on the highest Re number in the ISHVAC-COBEE workshop;[29] that is, indicating a fully developed turbulent flow.

The Archimedes number was defined as Ar $=(\beta g H \Delta T_0)/u_0^2$, with β the thermal expansion coefficient, g the gravitational acceleration and ΔT_0 the temperature difference between the average temperature at the return below the right wall (see red dashed line in Figure 1) and the temperature at the supply opening.

The heat input provided by the user at the heated wall determines the corresponding Ar, based on ΔT_0; that is, the difference between the average temperature at the return and the temperature at the supply opening. The participants were advised to study a range of heat fluxes between 0 and 100 W/m^2 to remain within the range of appropriate Ar numbers (0 < Ar < 8). Finally, the participants were asked to check that an outflow could be found only at the return "line/surface" (ie, that the flow was directed only toward the outlet opening).

2.1.3 | Parameters of interest

The first value to be considered by the participants was $x_{re}/(H − h)$, the dimensionless length from the heated end wall to the location of reattachment, that is, where the reattached flow was separated into a flow back to entrainment into the wall jet and a forward flow toward the outlet (Figure 1). The length x_{re} is commonly referred to as the penetration length of the supply jet. The second parameter of interest was the dimensionless maximum velocity in the "occupied zone": u_{rm}/u_o, where u_0 is the inlet velocity, that is, the maximum velocity in the return flow where the streamlines are close (below the center of the large recirculation cell; see Figure 1). The exact position of this parameter was potentially more difficult to determine;

however, the value of u_{rm}/u_o showed only small variation in the direction of the flow and thus had a limited impact. The distance from the heated wall to the location of the maximum velocity u_{rm} was x_{rm}, the third parameter compared, which was again made dimensionless using the room height H and the supply slot height h: $x_{rm}/(H − h)$. The main focus of this study was penetration length ($x_{re}/(H − h)$); additional results are included in Appendix S1.

2.2 | Participants

The participants invited by the workshop organizers were researchers, scientists, and consultants from universities, research institutes, and companies. Everyone in the CFD community was able to join,
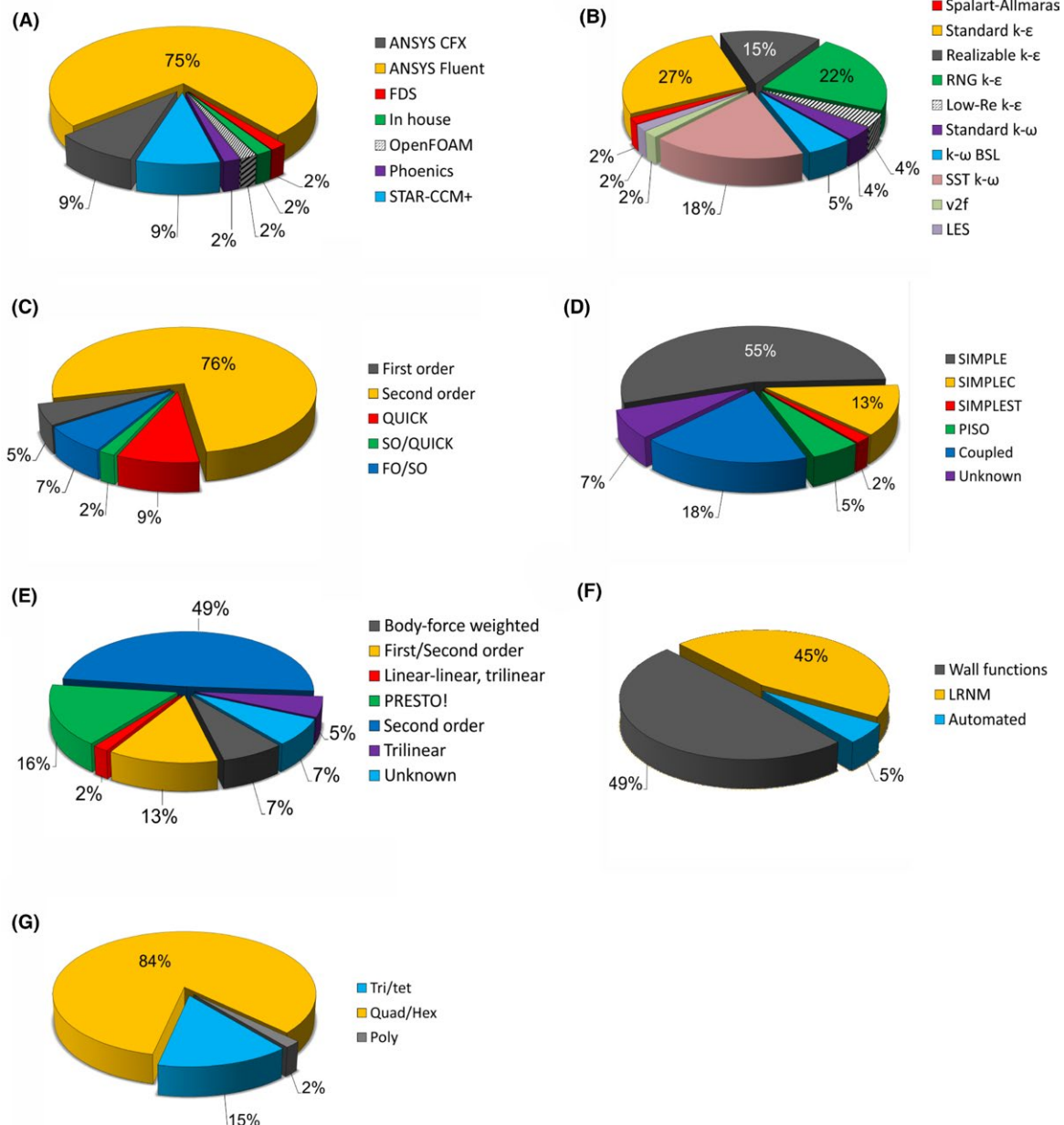

FIGURE 2 Subdivision of submissions by A, computational fluid dynamics (CFD) code; B, turbulence model; C, discretization scheme; D, solution algorithm; E, pressure interpolation scheme; F, near-wall treatment; G, grid type

and participation was on a voluntary basis. All were professionally active in CFD for indoor airflow, but of course, the level of experience in CFD depended on—among other things—the age and position of each participant. A five-page description of the flow problem (see Section 2.1) was provided to the participants, and they were asked to choose a CFD code (commercial or self-developed). They were also free to select a turbulence model, near-wall treatment, grid type, discretization scheme, etc. It is important to stress that simulating the flow problem provided was certainly not an easy task; the flow problem is challenging, no experimental data was provided for comparison, and there was no contact between the participants during the execution of the simulations prior to the workshop presentation at Indoor Air 2016.

Random numerical codes ranging from C1 to C32 were assigned to the teams to ensure that the results were treated anonymously. Teams that submitted more than one set of simulations, as in cases of repeated simulations with two or more turbulence models, had a letter appended to their team number (eg, C7a, C7b). Each team was asked to submit predictions of $x_{re}/(H - h)$, $x_{rm}/(H - h)$ and u_{rm}/u_0, for at least six Archimedes numbers between 1 and 8. A template was provided for the participants to specify the parameters and settings for their simulations, such as the CFD code, choice of turbulence model, discretization scheme, solution method, dimensions (2D or 3D), boundary conditions, near-wall treatment, grid type and size, convergence criteria, and number of iterations. Finally, the participants were asked whether they had used CFD guidelines when making decisions on the model setup, and whether a grid-sensitivity analysis had been performed.

2.3 | Submissions

The 32 teams submitted their results by the deadline of June 1, 2016, and the results were subdivided into 55 simulation datasets. The participants came from all over the world, with the majority from Europe and Asia. Various CFD codes were used, but the commercial CFD code ANSYS Fluent was the most popular, used by 75% of the participants (Figure 2A). Nine Reynolds-averaged Navier-Stokes turbulence models were used, and one submission consisted of a large eddy simulation (LES) using Fire Dynamics Simulations software (C30c) (see Figure 2B). The majority of the simulations were conducted with the k-ε family of turbulence models (69%), of which the standard k-ε model[30] and the RNG k-ε model[9] were the most popular, representing 27% and 22% of the total. The shear stress transport (SST) k-ω model proposed by Menter[11] was the third most popular model, used by 18% of the participants, followed by the realizable k-ε model,[10] at 15%. The other turbulence models, Spalart-Allmaras,[31] a low Reynolds number version of the k-ε model,[32] the k-ω baseline (BSL) model,[11] the standard k-ω model,[12] the v^2-f model,[33] and LES, did not have significant shares; that is, their percentages were below 5%. Figure 2C depicts the subdivision of the submissions with respect to the choice of discretization scheme. The vast majority (76%) of the teams used second-order discretization schemes for their simulations, and the second largest proportion

(9%) used the QUICK scheme. Only 5% of the submissions were based on first-order discretization schemes. The use of second- or higher-order discretization schemes has been recommended by—among others—Casey and Wintergerste,[18] Chen and Srebric,[19] Nielsen,[21] Nielsen et al,[22] and van Hooff and Blocken.[34] The participants used both coupled and segregated solvers. In the segregated solvers, algorithms such as SIMPLE, SIMPLEC, SIMPLEST, and the PISO scheme were used for pressure-velocity coupling. Figure 2D shows that the SIMPLE scheme was used most often by the participants, with a share of 55%, followed by coupled solvers (18%) and SIMPLEC (13%). Figure 2E shows that the majority of the participants used second-order pressure interpolation (49%), while Figure 2F shows that wall functions and LRNM were about equally often employed. Finally, Figure 2G shows that the majority (84%) of the participants constructed a structured (non-uniformly spaced) grid (quad/hex).

The participants were asked to report whether guidelines had been used to set up their computational models (eg, to choose a turbulence model, discretization scheme or grid resolution). Although the majority of the teams did not report using guidelines, they may in fact have used such guidelines to a limited extent, and/or their decisions may have been indirectly based on the use of such guidelines in the past. The use of guidelines and other reference documents was explicitly reported by teams C1 (REHVA handbook[22]), C6,[19] C7 (own experience and validation studies), C16 (ANSYS Fluent manual, own experience and the COST Best Practice Guideline), C17 (OpenFOAM user guide), C21a,b[18,35]), and C29a-c (ANSYS Fluent user guide). The influence of the use of guidelines is analyzed in Section 3.5.

Figure 3A,B provides two examples of the grids used for the simulations. Both are structured grids, but they show different grid-point clustering in the computational domain. Figure 3C,D shows the grid sizes used by all of the groups, subdivided according to whether a grid-sensitivity analysis was used (Figure 3C) or not used (or not reported to be used) (Figure 3D). Grid-size distribution was relatively similar for the two groups, although the grids not based on a grid-sensitivity analysis appeared to be slightly larger on average. Grid-sensitivity analysis has the potential to yield an optimum grid resolution, sufficiently fine to obtain (nearly) grid-independent results, without creating excessively large grids. Figure 3A also shows that no consensus was achieved on the appropriate grid size based on a grid-sensitivity analysis, with a very large variation in the number of cells used in the 2D simulations: from 1100 to about 1 million.

3 | RESULTS

3.1 | Overall

Fifty-five sets of simulation results were submitted by 32 teams. An overview of the results by $x_{re}/(H - h)$ value is provided in Figure 4A. First, the results showed a very large spread. Second, a clear dependence on the chosen turbulence model, and even model family, was observed. The yellow symbols in Figure 4A indicate predictions made using the k-ε family of turbulence models, that is, the standard
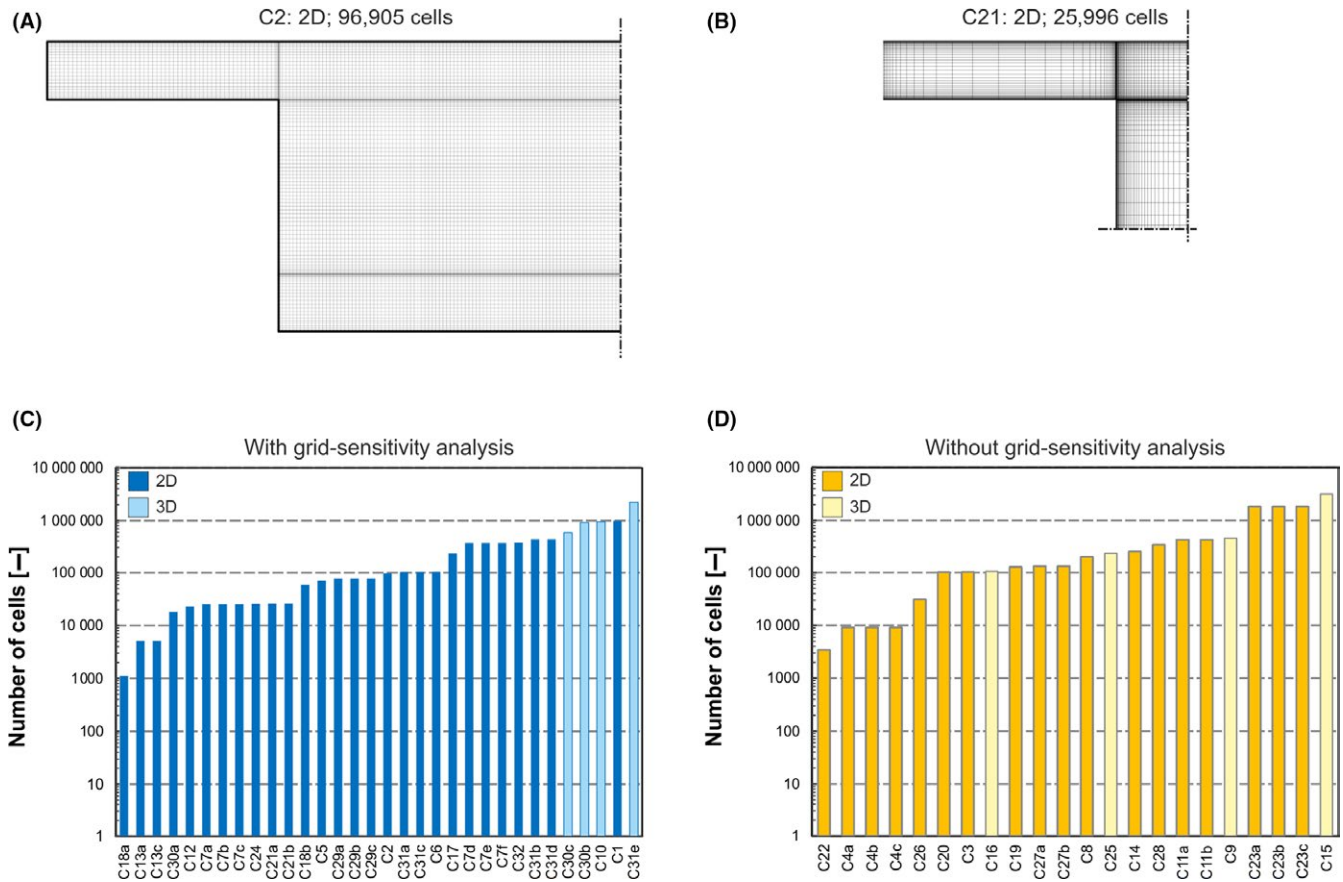
FIGURE 3 A, B, Grids around the inlet used by (A) team C2 and (B) team C21. C, D, Grid sizes used by the participants (C) with grid-sensitivity analysis and (D) without grid-sensitivity analysis

k-ε model, the RNG k-ε model, the realizable k-ε model, and the low Reynolds number version of the k-ε proposed by Chang et al;[32] and the black symbols indicate predictions made with the k-ω family of turbulence models, that is, the standard k-ω model, the SST k-ω model, and the k-ω BSL model. The majority of the results obtained using the k-ε models fell between $4 < x_{re}/(H − h) < 8$, whereas the k-ω models tended to predict values of $x_{re}/(H − h)$ between 10 and 12. Figure 4A shows that some of the values of $x_{re}/(H − h)$ obtained using the RNG k-ε and realizable k-ε models were also situated between 10 and 12, whereas all values of $x_{re}/(H − h)$ obtained using the standard k-ε model were below 8. Therefore, a fundamental albeit not universal difference was observed in the predicted values of $x_{re}/(H − h)$ between the two eddy-viscosity turbulence model families most often used for indoor airflows: k-ε and k-ω. Section 3.2 provides a more detailed analysis of these apparent differences. For the actual flow, one of the turbulence models was expected to be favorable for a solution, but only benchmarking could clarify the selection of a model. Interestingly, the spread observed at Ar = 0 was similar to the high Re case reported by Peng et al.[29] In addition, the spread did not seem to have been affected by Ar. In addition to differences in grid resolution and type, near-wall treatment, discretization schemes, convergence criteria, etc., the use of different initial conditions may have been responsible for the differences observed in the results obtained using identical turbulence models. As indicated by Nielsen

et al,[36] different solutions to a non-isothermal flow problem may be obtained when performing similar simulations with different initial conditions (increasing vs decreasing Ar). Schwenke[37] made a similar observation in experiments based on the flow configuration also studied by Nielsen et al.[36]

Figure 4B suggests that the spread of the distance x_{rm} was also unaffected by the Archimedes number, which indicates that the flow pattern was similar for all Ar numbers. This effect may indicate that the variation in the gravity forces (Ar numbers) in the predictions was small compared to the selected supply momentum (Re number). Figure 4C does show changes in dimensionless flow velocity as a function of the Archimedes number, but only up to a velocity level u_{rm}/u_o of 1.0-1.2, compared with an isothermal level of 0.3-0.6. Predictions with much larger Archimedes numbers or much smaller Reynolds numbers may clarify these observations.

3.2 | Turbulence models

This analysis focuses on the k-ε and k-ω families of turbulence models, which were used by about 95% of the participating teams. Figure 4 shows that the results obtained using the k-ε models can generally be distinguished from those obtained using the k-ω models. Two stages of statistical analysis were conducted to assess this difference in more detail. First, first-order statistics were calculated,
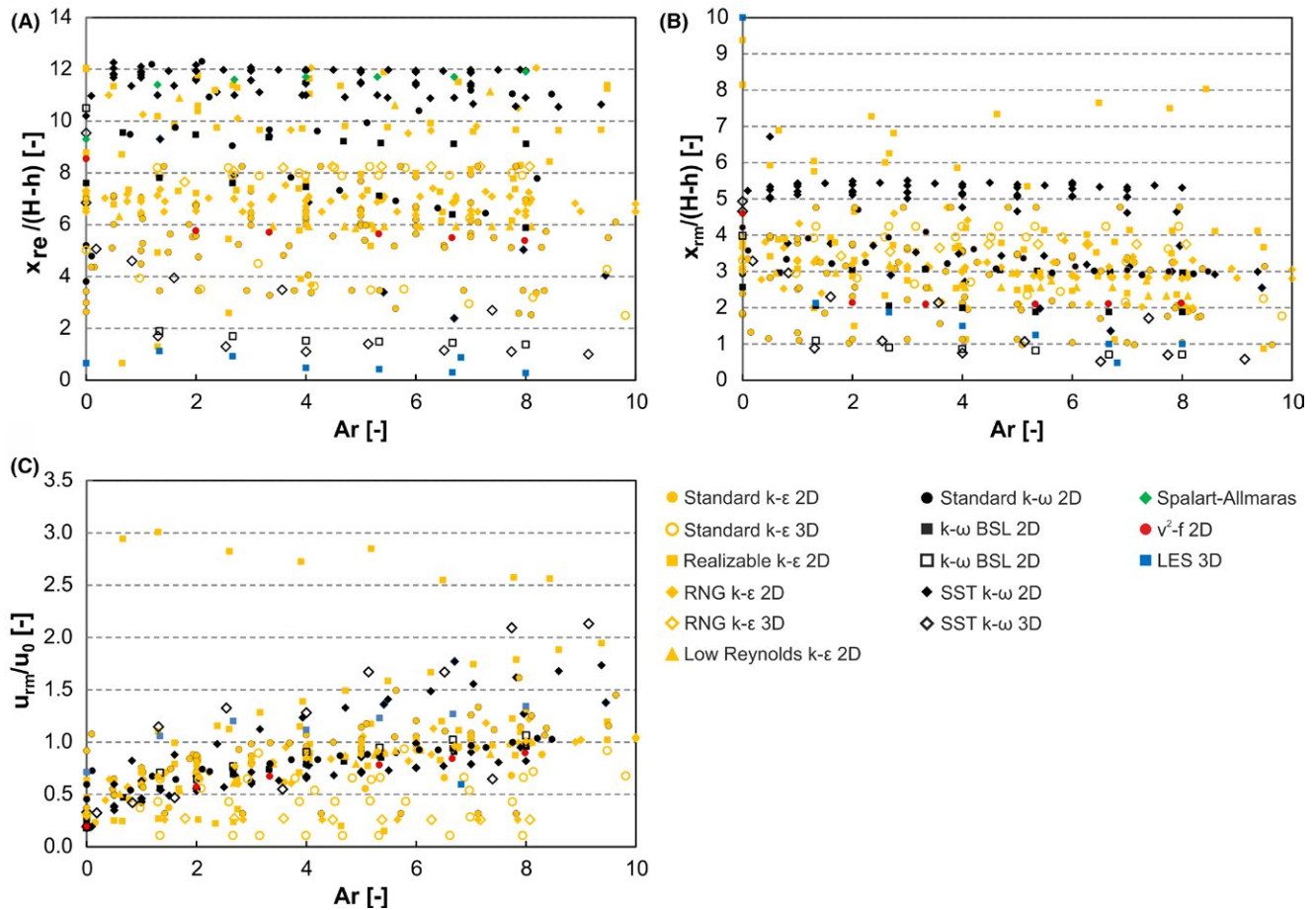
FIGURE 4 Results as function of Archimedes number (Ar) subdivided by turbulence model. A, $x_{re}/(H-h)$. B, $x_{rm}/(H-h)$. C, u_{rm}/u_o

a frequency distribution table was constructed from these statistics using specific class widths, a probability density function (PDF) of the normal distribution was plotted in a graph, and a histogram was plotted based on the frequency distribution. Second, a *t* test was used to determine whether the differences between the results for the k-ε and k-ω models were significant. The results of both stages of analysis were grouped with respect to the Ar number: (a) 0 < Ar < 3.5; (b) 3.5 < Ar < 7; and (c) 7 < Ar < 10. Note that Ar = 0 was not included; this was regarded as a separate class due to the absence of thermal effects. The Ar range chosen for each group ensured enough data to allow a statistical analysis for each group.

3.2.1 | Frequency distribution and PDF

The spread of the results for the k-ε and k-ω turbulence model families was analyzed with respect to the three parameters of importance: $x_{re}/(H-h)$, $x_{rm}/(H-h)$ and u_{rm}/u_0. This section provides the results for $x_{re}/(H-h)$; the results for $x_{rm}/(H-h)$ and u_{rm}/u_0 can be found in Appendix S1. Figure 5 shows the histograms and PDFs for the results obtained for (A, B) 0 < Ar < 3.5; (C, D) 3.5 < Ar < 7; and (E, F) 7 < Ar < 10. The most important observation was that the average values for $x_{re}/(H-h)$ were lower for the k-ε models than for the k-ω models for all three ranges of Ar number. In addition, the

results obtained using the k-ε models generally fitted a normal distribution, while those obtained using the k-ω models did not, due to the wide spread in the results (1 < $x_{re}/H-h$ < 12.25). For all ranges, the standard deviations σ (depicted in the graphs) were lower when a k-ε model was used. In addition, Figure 5B,D,F shows that the values of $x_{re}/(H-h)$ almost reached the maximum possible value of 12.5, indicating that in several of the simulations conducted using a k-ω model, the room was not long enough to allow detachment. Figure 5B,D (0.0 < Ar < 7.0) indicates that the mean penetration length may even have been larger.

3.2.2 | Independent *t* test

The independent *t* test was used to assess whether the differences observed between the results for the k-ε models significantly differed from those for the k-ω models. The confidence interval was 95%. The subdivision used as a function of Ar in Section 3.2.1 was used. Table 1 shows the values obtained. Significant differences (Sig. [two-tailed] < 0.05 in Table 1) in $x_{re}/(H-h)$ were found between 0 < Ar < 3.5 and 3.5 < Ar < 7. These significant differences are also depicted in the figures in the previous section. The parameter $x_{re}/(H-h)$ seemed to be quite sensitive to the choice of turbulence model family. Again, it should be noted that the penetration lengths
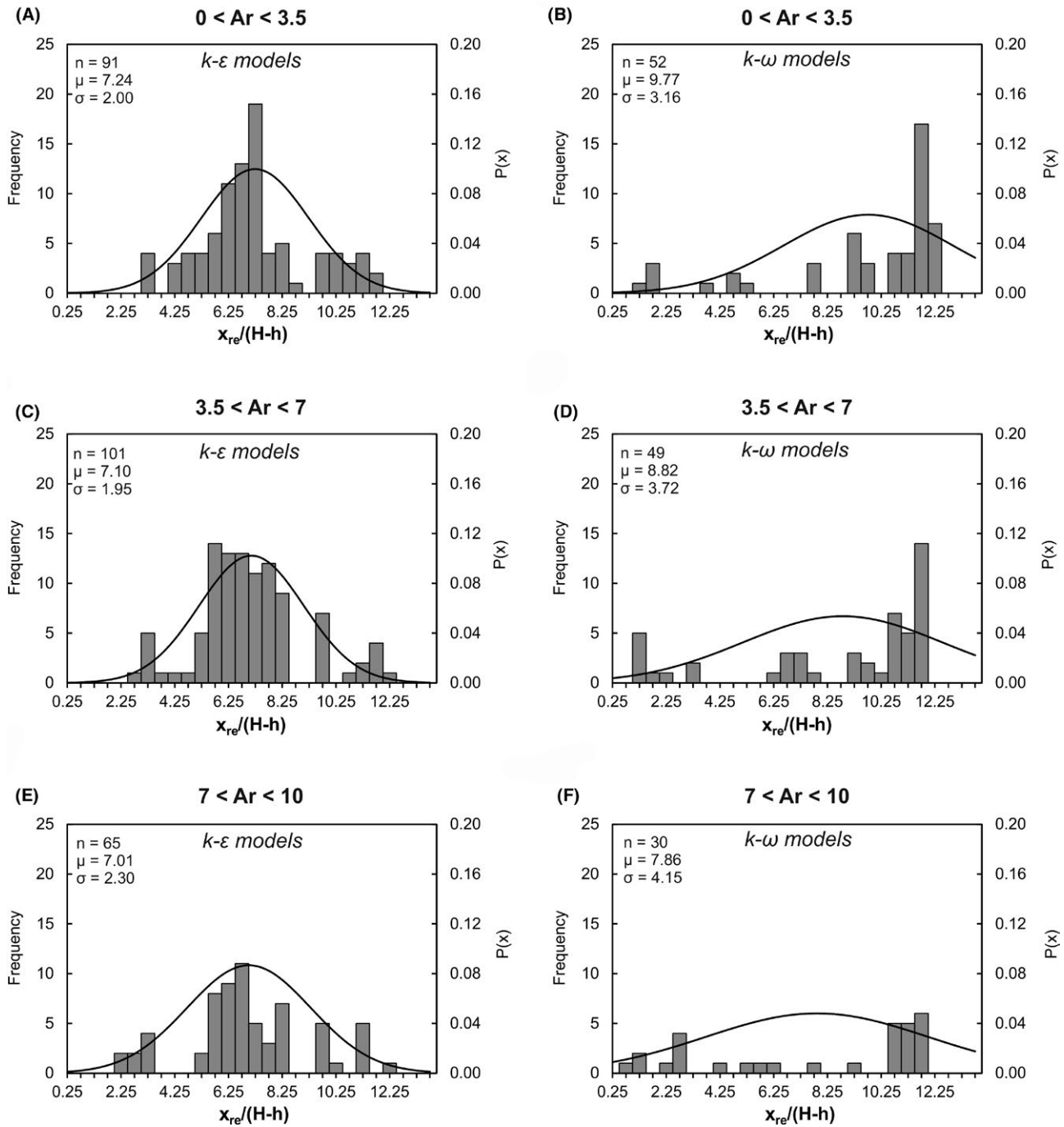
FIGURE 5 Histogram and related normal distribution of $x_{re}/(H - h)$ for the k-ε and k-ω models: (A, B) 0 < Ar < 3.5; (C, D) 3.5 < Ar < 7; and (E, F) 7 < Ar < 10

predicted by the k-ω models were near the border of the computational domain, indicating that the chosen domain length was too short and that a longer domain length might have resulted in larger differences in predicted penetration length.

3.3 | Near-wall treatment

The type of near-wall treatment that can be used depends on the grid resolution near the wall. If the grid is fine enough in the wall-adjacent

region (dimensionless wall distance y^* [or y^+] < 5 and preferably around 1), LRNM can be applied, solving the flow all the way down to the viscous sublayer. If the grid is coarser (y^* > 20-30), wall functions must be applied, with semi-empirical equations used to bridge the gap between the wall and the center of the wall-adjacent cell. LRNM provides more accurate predictions of the boundary layer flow and separation and heat and mass transport in this region.

Figure 6 shows the participants' results subdivided by the type of near-wall treatment. In some cases, an automated wall treatment

TABLE 1 T test scores: comparison of results of simulations using k-ε models and k-ω models

| Ar | Levene's test for equality of variances | | T test for equality of means | | | | | 95% Confidence interval for the difference | |
	Sig.	Equal variances	T	df	Sig. (two-tailed)	Mean difference	SE difference	Lower	Upper
0 < Ar < 3.5	0.002	Not assumed	−5.2	74.8	0.000	−2.5	0.49	−3.5	−1.6
3.5 < Ar < 7	0.002	Not assumed	−3.0	61.1	0.004	−1.7	0.57	−2.8	−0.6
7 < Ar < 10	0.002	Assumed	−1.3	93.0	0.202	−0.85	0.66	−2.2	0.5

was reported in combination with y^* values in the range of both wall functions and LRNM; these results are excluded from the figures. No clear conclusions can be drawn from Figure 6. The results showed a large spread in all categories of near-wall treatment, especially for the k-ε turbulence models, with $3 < x_{re}/(H − h) < 12$ (Figure 6A). For the k-ω models, the spread was smaller, with $6 < x_{re}/(H − h) < 12$ in general (Figure 6B). Evidently, the type of near-wall treatment was just one of many settings that influenced the results. Furthermore, several kinds of LRNM are available for near-wall flow, usually depending on the turbulence model chosen. For example (at least in Fluent), high Reynolds number versions of the k-ε model (standard, RNG, realizable) use a two-layer model in which the near-wall region is subdivided into (a) a viscosity-affected region and (b) a fully turbulent region using a wall distance–based turbulent Reynolds number Re_y. In a viscosity-affected region ($Re_y < 200$), Wolfshtein's[38] one-equation model is used. As a result, the momentum equations and the transport equation for the turbulent kinetic energy (k) are maintained, while no transport equation is solved for ε (turbulence dissipation rate). The values of ε are calculated based on a simple relationship between turbulent kinetic energy and a certain length scale. Low Reynolds number versions of the k-ε model consist of

transport equations for both turbulent kinetic energy (k) and turbulence dissipation rate (ε), and use damping functions to improve the predictions near the wall, which depend on the type of low Reynolds number k-ε model chosen. Similarly, depending on the k-ω model chosen, more than one transport equation for turbulence is solved near the wall. Given the use of different approaches to model the near-wall region, even within a certain turbulence model family (k-ε or k-ω), the large spread in results is not particularly surprising.

Figure 7 shows the histograms and PDF for the results obtained using wall functions and LRNM for the following ranges: (A, B) 0 < Ar < 3.5; (C, D) 3.5 < Ar < 7; and (E, F) 7 < Ar < 10. For smaller Ar numbers, the average value of $x_{re}/(H − h)$ is lower when wall functions are used than when LRNM is used. In addition, standard deviations are lower when wall functions are used.

Figure 7A, C, and E to some extent resemble Figure 5A, C, and E, respectively, mainly because the majority of the participants who used wall functions also chose one of the k-ε turbulence models. In Figure 7B, D, and F, each histogram has two peaks: one around $x_{re}/(H − h) = 7$ and one around $x_{re}/(H − h) = 12$. These two peaks correspond to the use of either a k-ε or a k-ω turbulence model; LRNM was used in combination with both k-ε and k-ω turbulence models. As the
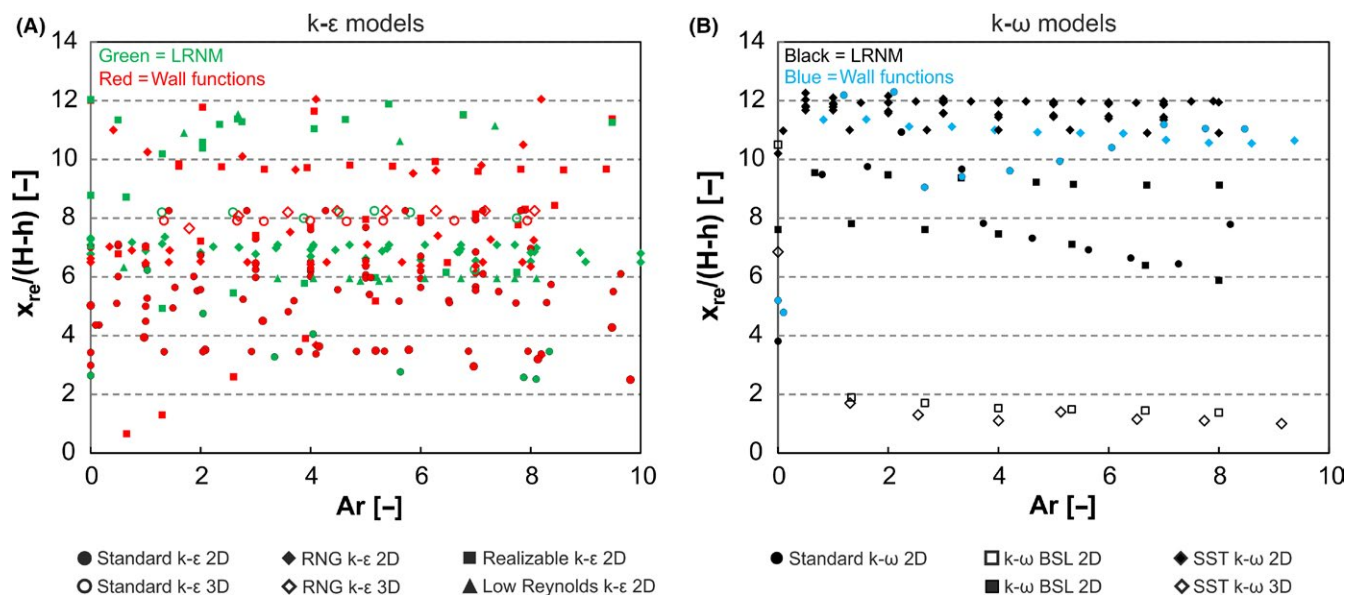
FIGURE 6 $x_{re}/(H − h)$ as a function of the Archimedes number (Ar). The results are subdivided based on the choice of near-wall treatment: A, k-ε model or B, k-ω model
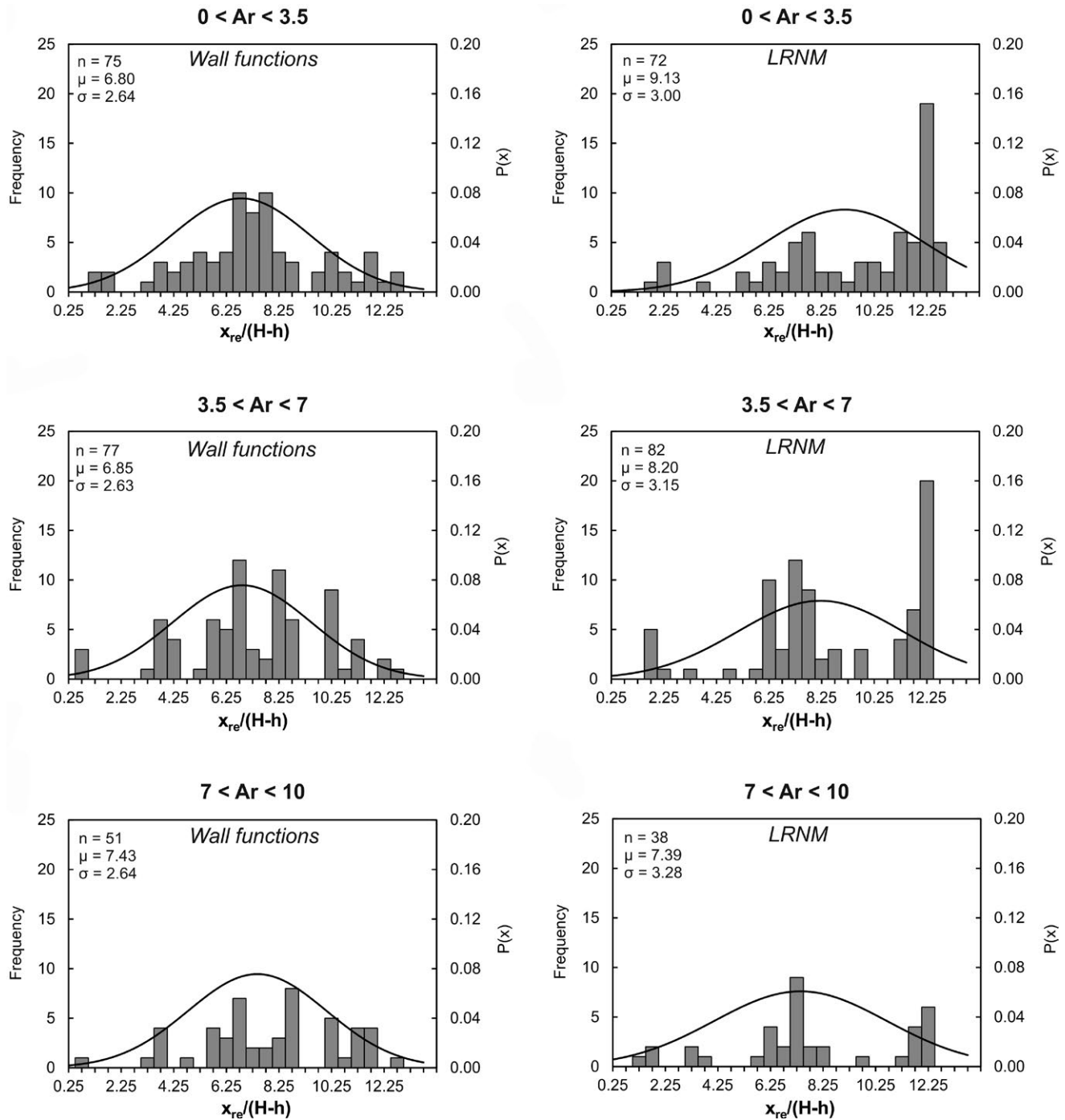
FIGURE 7 Histograms and related normal distribution of $x_{re}/(H - h)$ for the wall functions and low Reynolds number modeling (LRNM): (A, B) 0 < Ar < 3.5; (C, D) 3.5 < Ar < 7; and (E, F) 7 < Ar < 10

choice of near-wall treatment cannot be seen as independent of the choice of turbulence model, it is difficult to draw strong conclusions on the differences between the results obtained using wall functions and LRNM.

3.4 | Grid size

Figure 8 shows the results subdivided by grid size for all submissions that used 2D simulations with k-ε turbulence models. Grid size

was subdivided as follows: (a) <30 000, (b) 30 000-200 000, and (c) >200 000. No clear conclusions can be drawn from Figure 8 on the influence of grid size; as due to considerable variation, no clear trends are visible.

Table 2 shows the mean, standard deviation, and standard error of the mean for the results obtained from each simulation with grid sizes in one of the three grid-size categories. Interestingly, for 0 < Ar < 3.5 and 3.5 < Ar < 7, the standard deviation for $x_{re}/(H - h)$ was lowest for the coarsest grids (<30 000 cells). For example, for
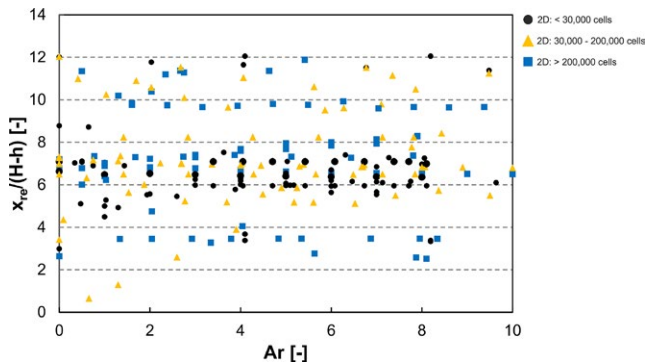
FIGURE 8 $x_{re}/(H - h)$ as a function of the Archimedes number (Ar) for 2D simulations with a k-ε model. The results are subdivided based on grid size

Archimedes numbers between 0 and 3.5, the standard deviation for $x_{re}/(H - h)$ was 1.3 for grids with fewer than 30 000 cells, but reached 2.8 and 2.4 for grids with 30 000-200 000 cells and more than 200 000 cells, respectively. The relatively limited spread in grid sizes with fewer than 30 000 cells is also clearly visible in the frequency distribution and associated PDF shown in Figure 9, with the smallest spread for the coarsest grids. However, the samples were relatively small. Unfortunately, no distinct relationships were found between grid size and parameters such as type of near-wall treatment.

3.5 | Use of guidelines

As mentioned in Section 2.3, 7 of the 32 teams reported using existing guidelines for the setup of their computational models. In this section, the results obtained by these teams are shown. As limited data are available for the teams that indicated using guidelines, the results are not subdivided by Archimedes number.

Figure 10 compares the results submitted by all of the participants with the results obtained by the teams that reported using CFD guidelines (best-practice guidelines, reference works, theory guides, etc.). The comparison reveals that the results submitted by the teams using guidelines showed less spread, especially those obtained from simulations with k-ε turbulence models. The standard

deviation for the overall results was 2.09, whereas that for the results based on guidelines was 1.24. Note that the mean value for the k-ε models was exactly the same, irrespective of the use of guidelines. Figure 10B and 10D show that the spread in the results of teams using guidelines was also smaller for the k-ω models, with a more pronounced clustering of results near $x_{re}/(H - h) \approx 12$, close to the downstream wall.

Turbulence models are well known to be developed primarily to solve flow problems with special conditions. However, successful models are often believed to be capable of solving flow problems in many other situations, which is not always correct. For a given flow situation, only one turbulence model is usually optimal; for example, see Zhang et al.[39]

Choosing an appropriate turbulence model for the geometry used in this study (for which experimental solutions were not known) can be achieved by finding experimental data (benchmarks) on flow problems similar to the situation addressed. Table 3 lists the penetration lengths measured for geometries with a specified h/H for Ar = 0 (isothermal case). The k-ε model appeared to be a good solution in this case, as for Ar = 0, $x_{re}/(H - h)$ was around 7, similar to the mean values obtained from the simulations with the k-ε turbulence models (see Figure 4A).

4 | CONCLUSIONS AND DISCUSSION

Those participating in the workshop at the 2016 Indoor Air Conference reported here were asked to perform CFD simulations of a non-isothermal flow problem for a range of Archimedes numbers (0 < Ar < 8). The analysis of the numerical results of the complex flow problem reported in Section 3 revealed a very large spread in the predicted dimensionless penetration lengths ($x_{re}/(H - h)$).

4.1 | Comparison with ISHVAC-COBEE workshop

This paper is based on a workshop at Indoor Air 2016, which focused on non-isothermal simulations for a range of Archimedes numbers, whereas a comparable workshop at the earlier ISHVAC-COBEE conference in Tianjin, China, focused on isothermal low Reynolds number flows.[29] The results for a Reynolds number of

TABLE 2 First-order statistics: comparison of $x_{re}/(H - h)$ from simulations with different grid sizes (#)

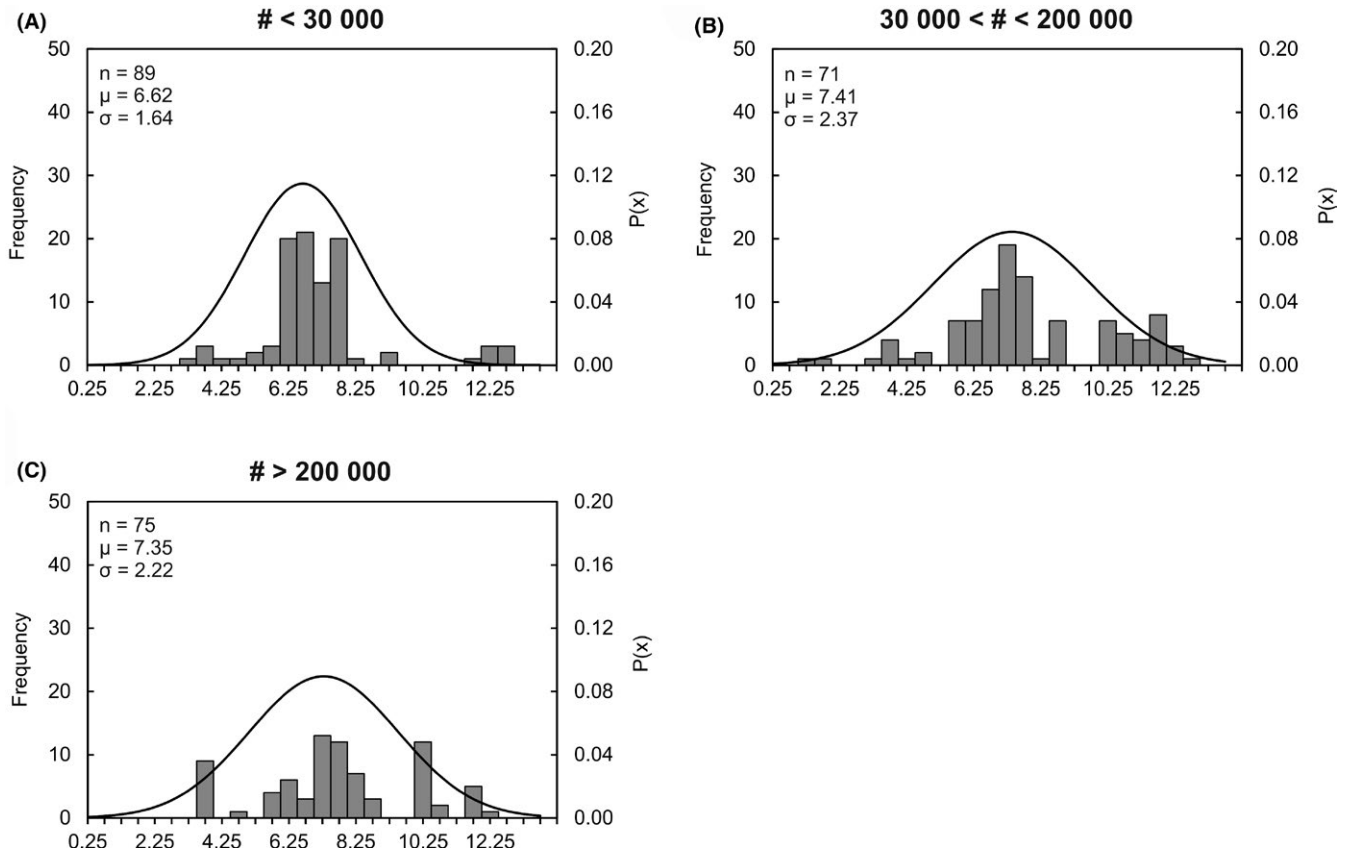| Ar	Grid size	N	Mean	SD	SE mean
0 < Ar < 3.5	# < 30 000	30	6.5	1.3	0.24
	30 000 < # < 200 000	25	7.0	2.8	0.57
	# > 200 000	31	7.5	2.4	0.43
3.5 < Ar < 7	# < 30 000	37	6.7	1.7	0.28
	30 000 < # < 200 000	27	7.2	2.0	0.38
	# > 200 000	26	7.2	2.4	0.46
7 < Ar < 10	# < 30 000	22	6.6	1.9	0.42
	30 000 < # < 200 000	19	8.2	2.1	0.49
	# > 200 000	18	7.3	1.7	0.41

FIGURE 9 Histograms and related normal distribution of $x_{re}/(H-h)$ for three grid sizes (averaged over all Ar > 0): A, # < 30 000; B, 30 000 < # < 200 000; and C, # > 200 000

10 000 showed a spread in $x_{re}/(H-h)$ of about 3-10, agreeing fairly well with the results of the workshop reported here: for Ar = 0, $x_{re}/(H-h)$ ranged from about 3 to 12 (see Figure 4A). Both cases showed a large spread, partly due to the use of different turbulence models (higher values for k-ω models than for k-ε models in both workshops). Figure 4A also shows that the spread in $x_{re}/(H-h)$ did not increase with the Ar number. Evidently, therefore, the addition of thermal effects did not increase the variation in the results. The choices made by the user in setting up such a model can be considered equally important in isothermal (Ar = 0) and non-isothermal (Ar > 0) cases.

4.2 | Turbulence models

It can be concluded from Sections 3.1 and 3.2 that the choice of a certain turbulence model strongly affects the flow pattern obtained. The values for $x_{re}/(H-h)$ obtained using the k-ε models clearly differed from those obtained using the k-ω models (Figures 4 and 5). As previously indicated, the majority of the results obtained using the k-ε models lay roughly in the range $4 < x_{re}/(H-h) < 8$, whereas most of the results of the k-ω models fell between $x_{re}/(H-h) = 10$ and $x_{re}/(H-h) = 12$, or were higher if a greater length had been defined for the flow domain. This seemed to indicate a fundamental difference in the predicted values of $x_{re}/(H-h)$ between the two most often used eddy-viscosity

turbulence model families: k-ε and k-ω (see Wilcox[12] for a theoretical introduction to both models). However, turbulence models do not provide an exact description of turbulence; they are closer to assumptions about turbulence in particular situations. It should also be noted that the spread in the results for each family of turbulence models (k-ε and k-ω), and even for specific turbulence models, was still significant, making it very difficult to generalize or draw clear conclusions from the results.

4.3 | Grid size

Figures 8 and 9 indicate the differences in the results for 2D simulations using a k-ε type turbulence model, subdivided into three grid sizes. Although the results showed a large spread, no clear conclusion can be drawn as to the influence of grid resolution, as no clear trends can be distinguished. This lack of correlation may be due to the combined effects of chosen grid resolution, turbulence model, and near-wall treatment, along with factors such as grid distribution and other computational settings. Surprisingly, approximately 58% of the grids used in the simulations were not chosen based on a grid-sensitivity analysis. However, Figure 3 shows that the actual grid size used was relatively independent of the performance of a grid-sensitivity analysis. Nevertheless, a grid-sensitivity analysis is a very important aspect of model verification and should not be neglected in research or consultancy. In addition, general guidelines for
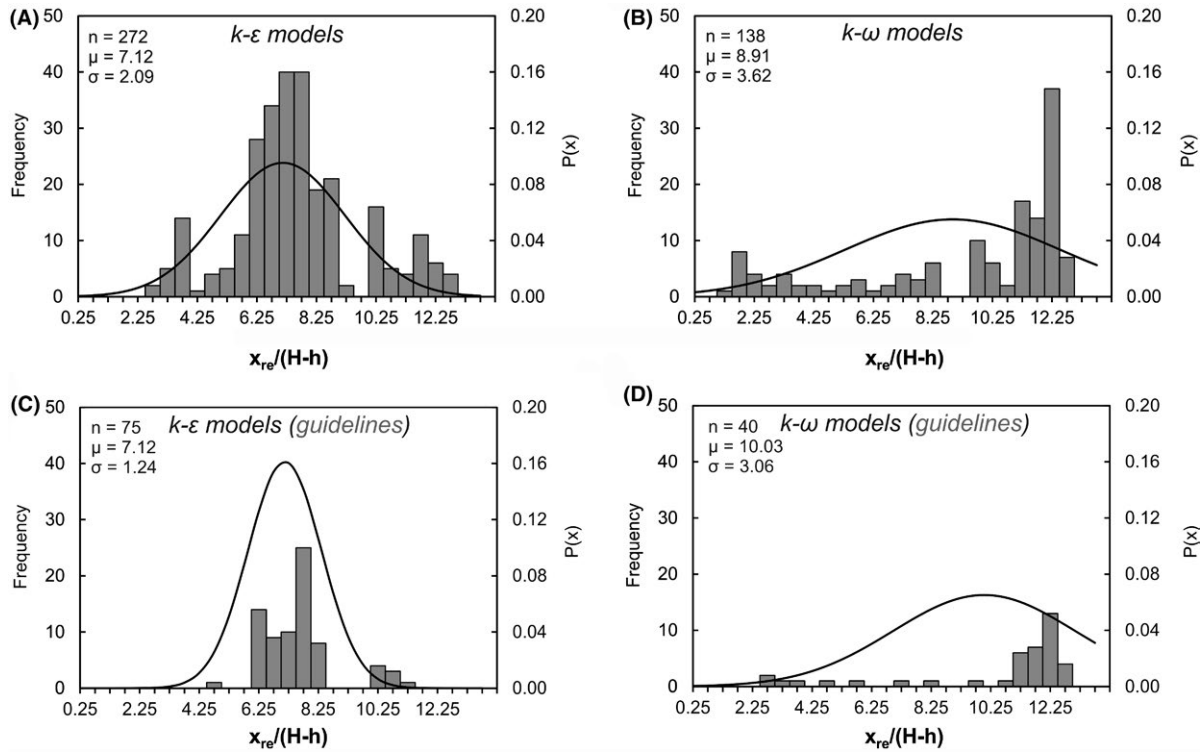
FIGURE 10 Histogram and related normal distribution of $x_{re}/(H - h)$ for simulations with and without the use of guidelines for the k-ε (A, C) and k-ω (B, D) models (average over all Ar > 0): (A, B) no guidelines used and (C, D) guidelines used

TABLE 3 Measured values of $x_{re}/(H - h)$ as a function of h/H ratio and Re_h

	$x_{re}/(H - h)$	Re_h	h/H
Restivo[43]	6.22	5000	0.17
Adams and Johnston[44]	7.3	100 000	0.6
Tihon et al[45]	6.8	2000	0.5
Tihon et al[45]	6.4	2000	0.4
Tihon et al[45]	7.0	2000	0.25

the appropriate dimensionless wall distance (y^* or y^+) for a certain near-wall treatment should of course be respected (wall functions: $y^* > 30$; LRNM: $y^* < 5$). Although insufficient information is available to draw firm conclusions, researchers using RANS are advised to (a) perform a grid-sensitivity analysis and (b) use non-uniform grids with spatially clustered cells in the boundary layers and other areas of interest to obtain a grid resolution suitable for LRNM without creating grids with excessively large grid-point counts.

4.4 | The use of CFD guidelines

Seven of the 32 teams reported using guidelines, such as their own validation studies, the REHVA guidebook of CFD simulations, journal papers, and CFD code manuals. The results obtained by the teams that reported using guidelines showed a smaller spread. This may be due to the assistance provided by the guidelines, although it is

impossible to say with certainty that those who did not report the use of guidelines failed to use guidelines at all, whether explicitly or implicitly. The participants who reported using guidelines may also have been more assiduous in their preprocessing and may generally have worked more conscientiously on their simulations. However, these are merely hypotheses; further research is needed to explain the observed differences.

4.5 | Ensuring the reliability of CFD models

The results of this workshop revealed that despite a considerable increase in computing power, the development of more sophisticated turbulence models, and a growing community of model users, the results of CFD simulations can show a very large spread, even when conducted by very experienced and well-trained CFD researchers, and should thus be handled with care. The user should specify a range of settings and parameters, all of which may influence the outcome of a CFD simulation. The choice of a certain turbulence model was found to have a very large effect on the outcome of the simulation (see Figure 4). User choice is further complicated by differences in the performance of turbulence models for different flow patterns, as shown in several publications;[39–41] no universal turbulence model performs best for all flow problems. The authors suggest that the ideal method is to perform a suitable and thorough validation study. When no validation data for the flow problem under study are available, researchers should use experimental datasets obtained for similar flow problems, that is, subconfiguration validation, as shown

in Section 3.5. Ensuring that a turbulence model can accurately predict the most important flow features increases confidence in the model's performance for the specific case under study, even when the geometry and/or ventilation configuration is slightly different. To the best of our knowledge, this methodology was not followed by many of the workshop participants, partly due to the limited time available for these kinds of scientific exercises. In addition to the turbulence model, the near-wall treatment employed showed to be an important factor. As the overall flow pattern can strongly depend on separation and surface-to-air heat transfer, it is advised to apply LRNM for indoor airflow problems (the type of LRNM depends on the choice for a certain turbulence model). Wall functions are far less accurate in predicting separation and heat transfer and should therefore not be used for most applications.

As the number of experimental datasets available was relatively limited, it is vitally important to increase the number of datasets that can be used for CFD model validation. Some experimental datasets are available at www.cfd-benchmarks.com and http://www.kbwiki. ercoftac.org/, and other datasets can be found in journal papers and other publications; however, it would be useful for the indoor CFD community to build and continuously extend a database of experimental datasets that can be freely used for CFD model validation. A similar database accompanied by best-practice guidelines is available for fire safety engineering problems in Denmark.[42] Although this is a different scientific research area, indoor airflow researchers working with CFD may benefit from adopting a similar approach for the benefit of future consultancy and research. The overall aims should be to reduce user influence as much as possible and to ascertain the accuracy and reliability of CFD solutions to indoor airflow problems. Education plays a crucial role here as well; the CFD community should strive for trustworthy and accurate CFD simulations of indoor airflows, and proper education of future engineers, consultants, and scientists is essential to achieve this goal.

ACKNOWLEDGEMENTS

ORCID

Twan Hooff http://orcid.org/0000-0002-7811-2745

Yuguo Li http://orcid.org/0000-0002-2281-4529

REFERENCES

1. Nielsen PV. Berechnung der Luftbewegung in einem zwangsbelüfteten Raum. *Gesund Ing.* 1973;94:299-302.
2. Nielsen PV. Prediction of the flow in air-conditioned rooms. Proceedings of the 14th International Congress of Refrigeration, Moscow, 1975.
3. Awbi HB. Application of computational fluid dynamics in room ventilation. *Build Environ.* 1989;24(1):73-84.
4. Jones PJ, Whittle GE. Computational fluid dynamics for building air flow prediction. Current status and capabilities. *Build Environ.* 1992;27(3):321-338.
5. Chow WK. Application of computational fluid dynamics in building services engineering. *Build Environ.* 1996;31:425-436.
6. Chen Q. Ventilation performance prediction for buildings: a method overview and recent applications. *Build Environ.* 2009;44:848-858.
7. Li Y, Nielsen PV. CFD and ventilation research. *Indoor Air.* 2011;21:442-453.
8. Nielsen PV. Fifty years of CFD for room air distribution. *Build Environ.* 2015;91:78-90.
9. Yakhot V, Orszag SA, Thangam S, Gatski TB, Speziale CG. Development of turbulence models for shear flows by a double expansion technique. *Phys Fluids.* 1992;4:1510-1520.
10. Shih TH, Liou WW, Shabbir A, Yang ZG, Zhu J. A new kappa-epsilon eddy viscosity model for high Reynolds-number turbulent flows. *Comput Fluids.* 1995;24(3):227-238.
11. Menter FR. Two-equation eddy-viscosity turbulence models for engineering applications. *AIAA J.* 1994;32:1598-1605.

12. Wilcox DC. *Turbulence Modeling for CFD*. La Canada, CA: DCW Industries, Inc.; 1998.

13. Roache PJ. Verification of codes and calculations. *AIAA J.* 1998;36(5):696-702.

14. Roache PJ. Quantification of uncertainty in computational fluid dynamics. *Annu Rev Fluid Mech*. 1997;29(1):123-160.

15. Stern F, Wilson RV, Coleman HW, Paterson EG. Comprehensive approach to verification and validation of CFD simulations – part 1: methodology and procedures. *J Fluids Eng*. 2001;123(4):793-802.

16. Oberkampf WL, Trucano TG, Hirsch C. Verification, validation, and predictive capability in computational engineering and physics. *Appl Mech Rev*. 2004;57(5):345-384.

17. Celik IB, Ghia U, Roache PJ. Procedure for estimation and reporting of uncertainty due to discretization in CFD applications. *J Fluids Eng*. 2008;130(7):078001.

18. Casey M, Wintergerste T. *Best Practice Guidelines. ERCOFTAC Special Interest Group on Quality and Trust in Industrial CFD*. Brussels: ERCOFTAC; 2000.

19. Chen Q, Srebric J. A procedure for verification, validation, and reporting of indoor environment CFD analyses. *HVAC&R Res*. 2002;8(2):201-216.

20. Sørensen DN, Nielsen PV. Quality control of computational fluid dynamics in indoor environments. *Indoor Air*. 2003;13(1):2-17.

21. Nielsen PV. Computational fluid dynamics and room air movement. *Indoor Air*. 2004;14:134-143.

22. Nielsen PV, Allard F, Awbi HB, Davidson L, Schälin A. *REHVA Guidebook No 10: Computational Fluid Dynamics in Ventilation Design*. Forssa, Finland: REHVA; 2007.

23. Johnson FT, Tinoco EN, Yu NJ. Thirty years of development and application of CFD at Boeing Commercial Airplanes, Seattle. *Comput Fluids*. 2005;34(10):1115-1151.

24. Krogstad PA, Eriksen PE. "Blind test" calculations of the performance and wake development for a model wind turbine. *Renew Energy*. 2013;50:325-333.

25. Krogstad PA, Sætran L, Adaramola MS. "Blind test 3" calculations of the performance and wake development behind two in-line and offset model wind turbines. *J Fluids Struc*. 2015;52:65-80.

26. Lockwood FC, Abbas T, Kandamby NH, Sakthitharan V. CFD experience on industrial combustors. *Prog Comput Fluids Dyn Int J*. 2001;1(1–3):1-13.

27. Baraldi D, Kotchourko A, Lelyakin A, et al. An inter-comparison exercise on CFD model capabilities to simulate hydrogen deflagrations in a tunnel. *Int J Hydrogen Energy*. 2009;34(18):7862-7872.

28. Rameshwaran P, Naden P, Wilson CA, Malki R, Shukla DR, Shiono K. Inter-comparison and validation of computational fluid dynamics codes in two-stage meandering channel flows. *Appl Math Model*. 2013;37(20):8652-8672.

29. Peng L, Nielsen PV, Wang X, Sadrizadeh S, Liu L, Li Y. Possible user-dependent CFD predictions of transitional flow in building ventilation. *Build Environ*. 2016;99:130-141.

30. Launder BE, Spalding DB. The numerical computation of turbulent flows. *Comput Methods Appl Mech Eng*. 1974;3(2):269-289.

31. Spalart P, Allmaras S. *A one-equation turbulence model for aerodynamic flows*. Technical Report AIAA-92-0439. American Institute of Aeronautics and Astronautics; 1992.

32. Chang KC, Hsieh WD, Chen CS. A modified low-Reynolds-number turbulence model applicable to recirculating flow in pipe expansion. *J Fluids Eng*. 1995;117(3):417-423.

33. Durbin PA. Separated flow computations with the k-ε-v^2 model. *AIAA J*. 1995;33(4):659-664.

34. van Hooff T, Blocken B. Low-Reynolds number mixing ventilation flows: impact of physical and numerical diffusion on flow and dispersion. *Build Simul Int J*. 2017;10(4):589-606.

35. Tu J, Yeoh GH, Lin C. *Computational Fluid Dynamics: A Practical Approach*. Oxford, UK: Butterworth-Heinemann; 2007.

36. Nielsen PV, Restivo A, Whitelaw JH. Buoyancy-affected flows in ventilated rooms. *Numer Heat Transfer*. 1979;2:115-127.

37. Schwenke H. *Das verhalten ebener horizontaler Zuluftstrahlen im begrenzten Raum*. Dissertation. Technical University of Dresden, Dresden, Germany, 1973.

38. Wolfshtein M. The velocity and temperature distribution of one-dimensional flow with turbulence augmentation and pressure gradient. *Int J Heat Mass Transf*. 1969;12:301-318.

39. Zhang Z, Zhang W, Zhai Z, Chen Q. Evaluation of various turbulence models in predicting airflow and turbulence in enclosed environments by CFD: part 2 – comparison with experimental data from literature. *HVAC&R Res*. 2007;13(6):871-886.

40. Zhai Z, Zhang Z, Zhang W, Chen Q. Evaluation of various turbulence models in predicting airflow and turbulence in enclosed environments by CFD: part 1 – summary of prevalent turbulence models. *HVAC&R Res*. 2007;13(6):853-870.

41. van Hooff T, Blocken B, van Heijst GJF. On the suitability of steady RANS CFD for forced mixing ventilation at transitional slot Reynolds numbers. *Indoor Air*. 2013;23:236-249.

42. Jakobsen A, Valkvist MBS, Bennetsen JC, et al. *CFD best practice*. Copenhagen, Denmark: Best Practice Gruppen; 2009.

43. Restivo AMO. *Turbulent flow in ventilated rooms*. PhD thesis, University of London (Imperial College of Science and Technology), London, 1979.

44. Adams EW, Johnston JP. Effects of the separating shear layer on the reattachment flow structure part 2: reattachment length and wall shear stress. *Exp Fluids*. 1988;6:493-499.

45. Tihon J, Penkavova V, Havlica J, Simcik M. The transitional backward-facing step flow in a water channel with variable expansion geometry. *Exp Therm Fluid Sci*. 2012;40:112-125.

SUPPORTING INFORMATION

Additional supporting information may be found online in the Supporting Information section at the end of the article.